

## Chapter 3

# Radio Frequency Sensor Modelling

### 3.1 Introduction

From the more general background and context shown in the previous chapter we now turn towards the more specific parts of Radio Frequency (RF) signal propagation physics and RF propagation models. Accurate RF sensor modelling can be a complex task but at the same time essential if the sensor model is to be used in a high-accuracy localisation application. The quality of the sensor model determines significantly the capability to achieve high-accuracy localisation. This chapter presents background information to RF sensor modelling.

The following points are presented in this chapter:

- The basic RF propagation mechanisms are described to give an understanding of the physical behaviour of electromagnetic signal propagation. Understanding the physical behaviour of a given sensor is essential in order to model it correctly.
- The topic of antenna radiation patterns is presented. Antennas form an integral part of any wireless communication application. The radiation pattern is essential as it shows the distribution of the emitted energy in all angular directions.
- Some important RF propagation models as they were developed are presented. Today they are predominantly used for communication purposes. It is argued that these models do not usually satisfy the requirements of sensor models used for high-accuracy localisation.
- To overcome the inadequacies of the RF propagation models used in communication applications, a few models have been specifically developed for mobile robot localisation. The most important of these models as they are used today are briefly presented.

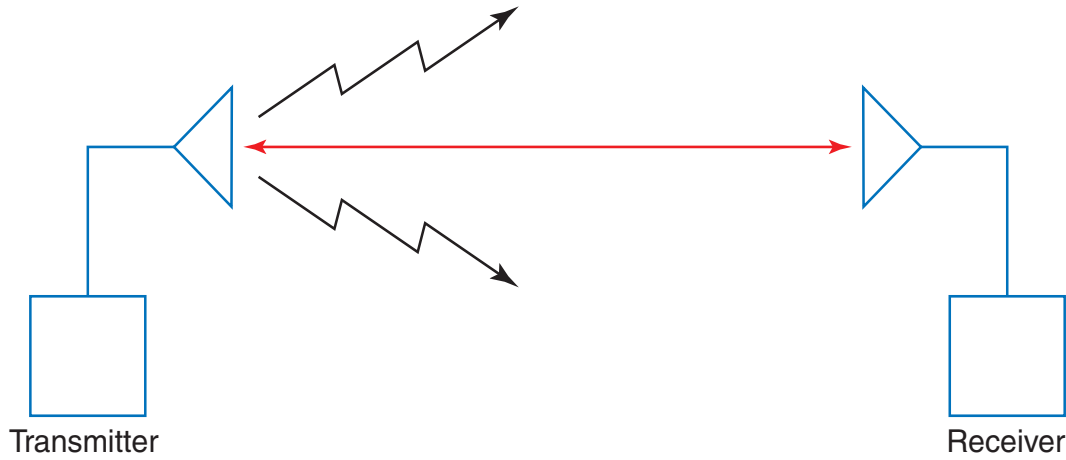


**Figure 3.1:** Wireless communication link — The typical components for a wireless communication link are the receiver and the transmitter with their corresponding antennas.

- Of the large variety of models available, two models are shown in more detail. The modified free-space model (*nth-power law*), where the received power decreases exponentially with the inverse of distance, is very popular for mobile robotics localisation applications. This model is described in more detail and serves for comparison purposes to a newly developed model in later chapters.

The two-ray model, which serves as a basis for the development of a new RF sensor model, is presented. It provides an understanding of the reasons why models used for mobile robot localisation to date are not sufficient to achieve high-accuracy localisation.

## 3.2 Radio Frequency propagation mechanisms

A typical RF communication link consists of a transmitter with corresponding transmitting antenna and a receiver with the receiving antenna, as shown in figure 3.1. Electromagnetic or RF waves emitted by the transmitter will propagate through the medium and then arrive at the receiver's antenna [53,90]. The characteristics of the antennas, the medium and some other factors discussed in the following section have a major influence on the amount of energy that will reach the receiver.

Path loss (or path attenuation) is commonly defined as the reduction in power density (attenuation) of an electromagnetic wave as it propagates through space and is of particular interest in this thesis as the received signal strength will be exploited to infer the distance between the receiver and the transmitter.

The Received Signal Strength Indicator (RSSI) is defined as the total received power

averaged over the bandwidth. Receivers provide the RSSI as a unit-less scalar value which can be converted into a power reading using a receiver specific formula provided by the manufacturer of the RF chip if needed. With increasing bandwidth, the fading effects affecting path loss and therefore also RSSI, as discussed later, become less prominent [92]. Fading of a channel can be summarised as the interference of different multipath contributions which result in time- and frequency-dependent fading and affect the gain of the channel. Accurate localisation using RF is challenging due to several factors influencing the propagation.

Electromagnetic waves such as RF waves propagate in a medium through the following mechanisms.

### Free space propagation

In free space, RF waves propagate radially from an emitter (point source). The ratio of received power  $P_{r,fs}$  to transmitted power  $P_{t,fs}$  as given in equation (3.1) is a function decaying with the square of the inverse of the distance  $d$  between transmitter and receiver. The wavelength of the transmission frequency is denoted using  $\lambda$ .

$$\frac{P_{r,fs}}{P_{t,fs}}(d) = \left( \frac{\lambda}{4\pi d} \right)^2 \quad (3.1)$$

### Reflection

Reflections occur whenever the RF signals encounter large objects in their path. Large in this context means more than a few wavelengths of the propagating electromagnetic wave. An example of such a reflection occurring from the ground surface is shown in figure 3.2. When reflections occur, the electromagnetic wave may be subjected to a phase shift. A complex reflection coefficient, usually labelled  $\Gamma$ , describes the change in gain when reflections occur at a surface. This coefficient is a function of the wavelength of the electromagnetic wave, the angle of incidence on the reflecting surface, the wave polarisation, and the reflecting material itself. Any RF based real world application, such as the Close Proximity System (CPS) has to deal with the effects of reflections, as reflections will always be present.

### Diffraction

If the RF signal path is obstructed by a surface with sharp edges, the waves will be diffracted. This has the effect that the waves will be present throughout the space, even behind the obstruction. Diffraction bends the waves and is the reason why waves are present even when a Line-of-Sight (LOS) path is not existent. One effect to keep in mind when designing a CPS

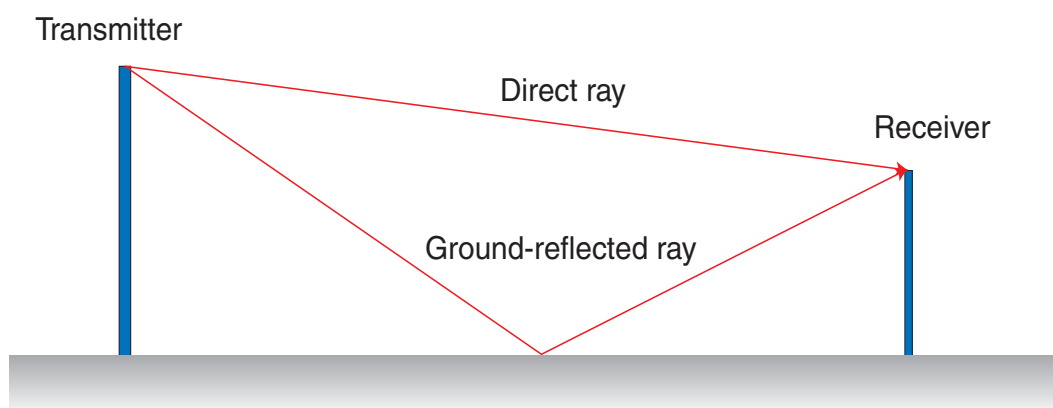


**Figure 3.2:** Reflection from the ground — The emitted rays arrive at the receiver via two paths: Line-of-Sight and reflection from the ground.

is that the effect of diffraction decreases with increasing electromagnetic wave frequency. This means that the likelihood of having blind spots for RF coverage is higher for higher frequencies than for lower frequencies. This issue becomes important when covering the area underneath a truck, where diffraction may play an important role in the propagation.

### Refraction

Refraction is the effect of a change in direction of a wave due to a change in velocity. This happens when a wave passes from one medium to another medium having a different refractive index. For RF communication this effect is encountered when the wave is refracted as it travels through the atmosphere, and can lead to a bent signal path. For long separation distances refraction is the main signal path for non-LOS communication. For a CPS operating at comparably short distances, and therefore presumably in areas with an almost constant refractive index of the propagation medium, this effect will most likely not be prominent.

### Scattering

Scattering occurs when the RF signals encounter small objects in their path. Small in this context means less than one wavelength in size. For example, rough surfaces, lampposts and street signs can induce scattering.

In real world applications the phenomena described in the previous subsections will not occur in isolation but manifest themselves at the same time with different magnitude. The signal intensity  $I$  at a receiver is the sum of all rays arriving through a potential multitude

of combinations of the above described effects. This can be described in a simplified form by equation (3.2). In this equation,  $a_k$  denotes the amplitude of the  $k$ th ray.

$$I = \sum_{k=1}^N a_k e^{i\omega t_k} \quad N \dots \text{number of rays} \quad (3.2)$$

### 3.3 Antennas

Antennas form an integral part of any RF communication link. Their radiation characteristics often influence the propagation of the RF waves through attenuation of certain directions. The typical theoretical radiation pattern of a short dipole (lambda quarter antenna) representative for the type of antenna built in the CPS hardware is presented in this section. The radiation pattern is used to demonstrate the effect of the mounting height of the antennas. This effect is important in a practical application.

#### 3.3.1 Radiation patterns

The two related quantities electric field, denoted  $E$ , and the power, denoted  $P$ , are of importance when describing the field pattern of any antenna. Antenna radiation patterns are drawn in Cartesian coordinates or polar coordinates and the radiation in any direction is described using the angles  $\theta$  and  $\phi$  [53]. The azimuth angle  $\phi$  is measured anticlockwise in the xy-plane with  $\phi = 0$  being the x-axis. Similarly, the elevation  $\theta$  is the angle between the z-axis and the xy-plane, where  $\theta = 0$  lies on the z-axis itself. Antenna patterns are often symmetrical with respect to one axis, as is the pattern of the lambda quarter antenna.

For the lambda quarter antenna aligned with the z-axis, the relative or normalised electric field pattern is described using equation (3.3).

$$\frac{E_\theta}{E_{\theta m}} = \sin \theta \quad (3.3)$$

Here the index  $m$  indicates the maximum value of the quantity, in this case the electric field. The corresponding relative power pattern is given by equation (3.4). The index  $n$  stands for normalised.

$$P_{\theta n} = \sin^2 \theta \quad (3.4)$$

The patterns of the electric field and power in the xy-plane and the xz-plane are shown in figure 3.3. In three dimensions, as shown in figure 3.4, the patterns form a doughnut shape. The variation of the pattern with the elevation angle  $\theta$  and the influence of this variation on the RSSI become important when the antennas of the CPS are installed at different heights.

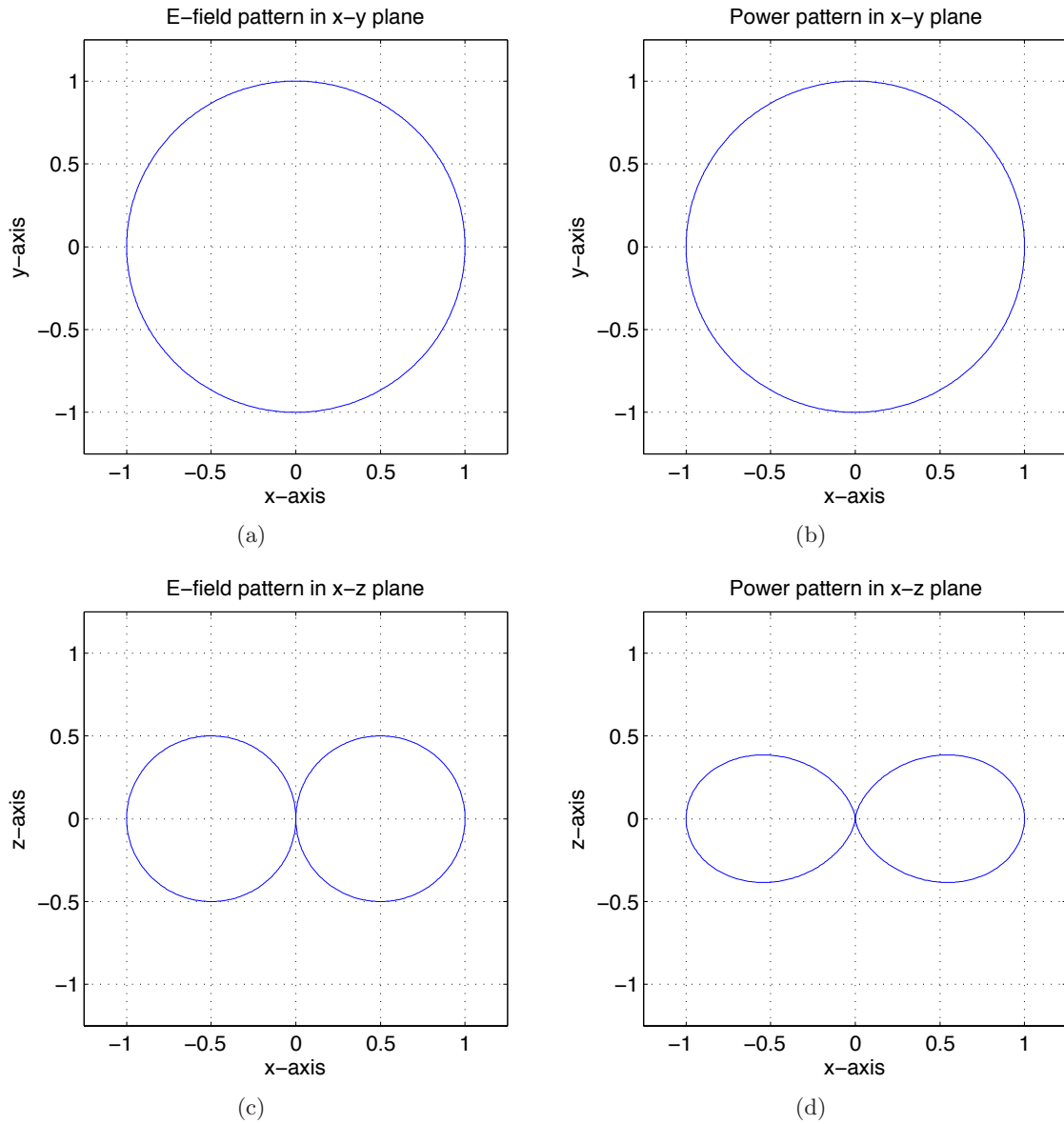


**Figure 3.3:** Antenna radiation patterns — The electric field and power patterns for the short dipole. (a) and (b) for the x-y plane and (c) and (d) for the x-z plane. These patterns vary only with the elevation angle  $\theta$  and are independent of the azimuth angle  $\phi$ . Therefore the patterns in the y-z plane are identical to those of the x-z plane.

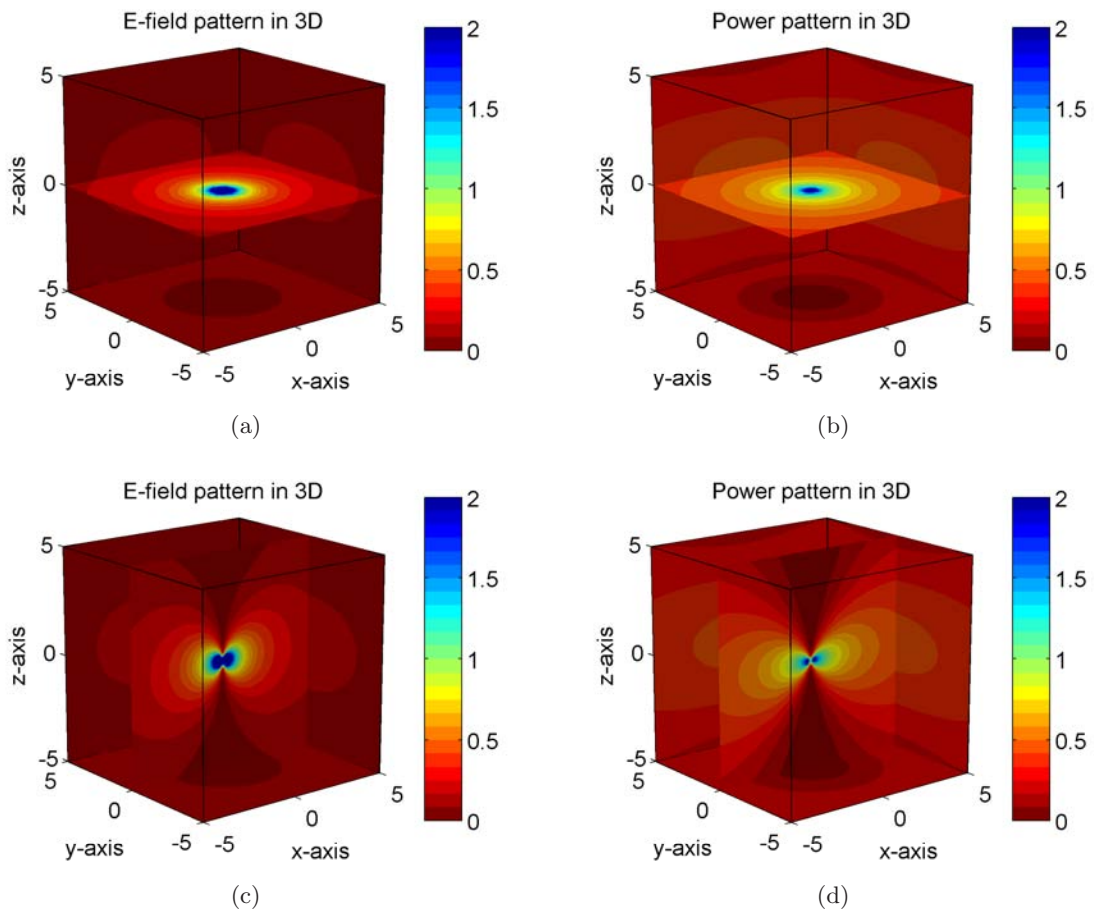


**Figure 3.4:** Antenna radiation patterns in 3D — A three dimensional representation of the electric field and power patterns for the short dipole. (a) and (b) for the x-y plane and (c) and (d) for the x-z plane.

### 3.3.2 Geometric considerations - the effect of mounting height

It was previously shown that antennas can exhibit directional gains. For a short dipole the power pattern is described using equation (3.4). This field has the property that the gain is maximum in the xy-plane independent of the azimuth angle and minimal in the z-axis direction. Depending on the mounting height and the distance between transmitter and receiver, this gain will change and influence the power of the individual rays with different magnitude. For example, each of the rays will be subjected to an individual antenna gain factor depending on the angle of radiation. For a given horizontal separation and mounting height of transmitter and receiver, the LOS ray will be subjected to a different gain from that of the ground-reflected ray, as shown in figure 3.5. There will be rays that are emitted with a low elevation angle (see the LOS ray of transmitter 1 in figure 3.5) and therefore will experience a higher gain than rays that are emitted at a large elevation angle (see the ground-reflected ray of transmitter 1 in figure 3.5). The influence of the antenna for the short dipole on the power pattern is described using equation (3.5)

$$G_a(\theta) = \sin^2 \theta \quad (3.5)$$

It should be noted that the gain  $G_a$  occurs at both the transmitter and the receiver antenna, making the total gain proportional to the square of the individual gains.

## 3.4 Models describing Radio Frequency propagation

The effects influencing radio frequency signal propagation manifest themselves in two different ways: firstly there is *Large Scale Fading*, which describes the effects when the distance between transmitter and receiver varies significantly, i.e. more than one wavelength, and secondly *Small Scale Fading*, which deals with the effects when the distance varies within less than one wavelength. The Antenna and Propagation community has put a lot of effort into the task of describing both of these effects [80, 86, 87].

Apart from this distinction, the models describing the propagation effects may also be divided into empirical models that deal with the statistical characterisation of the received signal, and site-specific models that take into account the physical conditions such as the geometry of the site. The difference between both is that the empirical models are usually easier to implement and are less sensitive to the environment, whereas the site-specific models are more accurate and usually computationally more expensive. As stated in [80] it is important to recognise that, when using an empirical model, the lack of knowledge of the system cannot be supplemented by a stochastic distribution. In other words, the need for a model is still present even when using a statistical model.

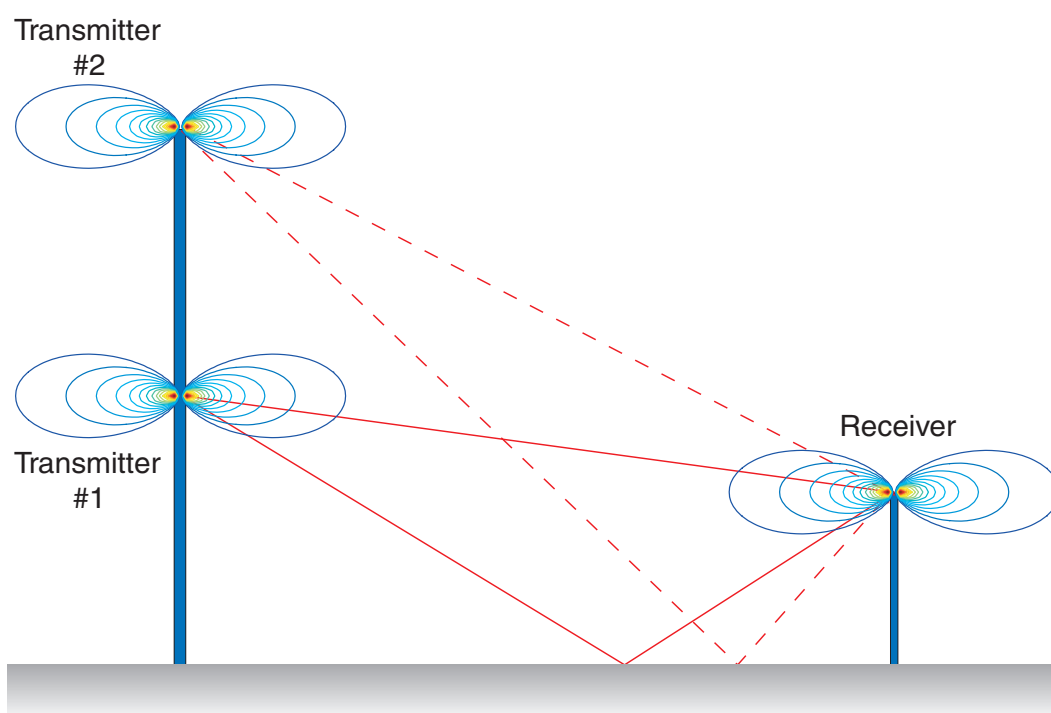


**Figure 3.5:** Schematic of the antenna influence — For big height differences between the transmitter and receiver even the LOS ray will be subjected to a small antenna gain (dashed line), leading to a small overall received power. The same effect occurs when the height difference is smaller and the separation distance is also small. In both cases the elevation angle of the LOS will be similar and therefore the gain will also be similar.

### Large scale fading

The main assumption for large scale fading situations is that one usually deals with macro-cells often with several tens of kilometres of separation between sender and receiver, thus often having no LOS conditions. This type of fading is due to motion over large areas. Its effects manifest themselves as a mean signal attenuation versus distance, with the occurrence of variations about the mean [86]. The statistics of this type of fading allows us to compute an estimate of the path loss as a function of the distance and is usually described using a mean path loss (*nth-power law*) and a log-normal distribution about the mean. Large scale fading models are mainly outdoor propagation models. In such scenarios, up to several tens of watts of transmission power is used, with the antennas placed high above the surroundings and the signal propagation is mainly by means of diffraction and reflection. For the size of these cells the refraction component may also be of importance.

### Small scale fading

Small scale fading effects manifest themselves as big changes in the signal amplitude and the phase. Statistical models are used to describe the changes in the envelope of the received signal. These models differ in the underlying assumptions they make about the signal paths between the transmitter and receiver. For example, the Rician distribution deals with the situation when there is a dominant LOS component, whereas the Rayleigh distribution describes situations with predominantly non-LOS signals. Another example is the Log-Normal Fading Model, which quantifies the distribution of signals undergoing multiple reflections and diffraction. These stochastic models need the signal mean which can be found from, for example, the two ray model, the three ray model, the multiple ray model or through ray-tracing techniques.

#### 3.4.1 *n*th-power law model - free space propagation model

A common model used for localisation applications is the *n*th-power law model (see for example [12]). The name *nth-power law* refers to the description given as

$$PL(d) = \frac{1}{d^n} \quad (3.6)$$

where the path loss  $PL$  decays with the inverse of the distance  $d$  to the power of  $n$ . The exponent  $n$  is the equivalent to the path loss factor  $\gamma$  as used in equation (3.10). The path loss factor can be found through regression of given data or from tables. It is important to notice that this model describes the large scale fading component only, which makes it difficult, if not impossible, to use it for high-accuracy mobile robot localisation. This will

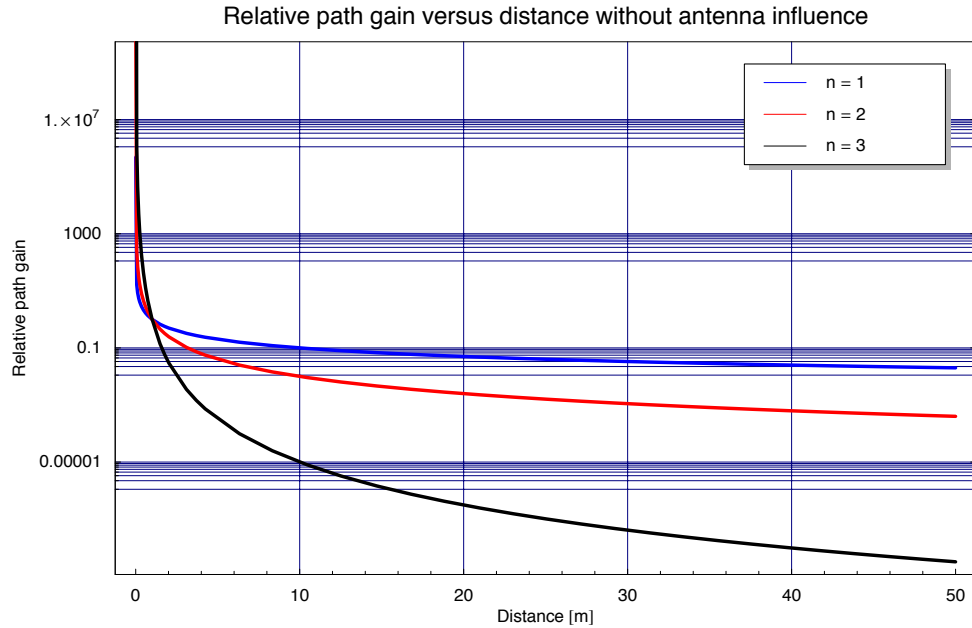


**Figure 3.6:** Relative path gain versus distance — Here shown for the  $n$ th power model and for three different path loss factors.

be shown in the next chapters. Figure 3.6 shows the path loss versus distance for different path loss factors.

### 3.4.2 Multiple-ray and two-ray model

The two-ray model is used in this thesis as the basis to argue the fact that the  $n$ th power model is often not accurate enough, or even incorrect, for localisation applications. Depending on the environment, considering two rays may not be sufficient and more rays may have to be taken into account. This is particularly true for urban environments where reflections from walls [68] are common, but it is not of such importance in open outdoor environments. With regards to the CPS application the two-ray model is now described, first without the influence of the antenna radiation pattern and following this, with the influence of the antenna.

#### Relative path gain for the two-ray model

The multiple-ray model can be seen as a simplified instance of the ray-tracing technique. This model calculates the path loss as it occurs due to the phase shift due to different individual path lengths from the transmitter to the receiver. It also takes into account the reflections as they occur on surfaces where paths other than the LOS signal will be reflected

(shown in figure 3.2). The relative path gain as a function of the distance for the multiple ray model can be described theoretically using equation (3.7) [97]. This model includes the free space loss in the first factor and the sum of the reflective components in the second factor. The two-ray model [13,35,60,96] is an instance of this general description for  $N = 2$  rays, one LOS ray and one usually ground-reflected ray.

$$P_r(d) = P_t \left( \frac{\lambda}{4\pi} \right)^2 \left| \sum_{i=1}^N \frac{\Gamma_i(\alpha_i)}{r_i(d)} \exp(-ikr_i(d)) \right|^2 \quad (3.7)$$

$$k = \frac{2\pi}{\lambda} \quad N \dots \text{Number of rays}$$

Here  $P_t$  and  $P_r$  stand for the transmitted power and the received power respectively, while  $d$  denotes the horizontal separation between transmitter and receiver. The ray length  $r_i$  is a function of this distance. The reflective coefficient  $\Gamma$ , equation (3.8), depends on the angle of incidence  $\alpha$  of the ray as well as on the properties of the reflecting material, which are described by  $\varepsilon_r$ , the relative dielectric constant.

$$\Gamma(\theta) = \frac{\cos \theta - a\sqrt{\varepsilon_r - \sin^2 \theta}}{\cos \theta + a\sqrt{\varepsilon_r - \sin^2 \theta}} \quad \text{where } \theta = 90 - \alpha \quad (3.8)$$

The constant  $a$  depends on the polarisation plane and is obtained as

$$a = 1 \quad \text{horizontal polarisation}$$

$$a = \frac{1}{\varepsilon} \quad \text{vertical polarisation}$$

The signal shown in figure 3.7 depicts the relative path gain for a received signal for the two-ray model composed of two components as shown in figure 3.2. This signal is the sum of the free space loss and the reflective components, but does not take into account any influences from the antenna radiation pattern.

The consideration of just one additional ray, as opposed to the  $n$ th power model previously presented, leads to significant changes in the path loss curve. Whereas the  $n$ th power model showed a monotonically decreasing characteristic with increasing distance, the two-ray model, and in general the multiple-ray model, shows a completely different behaviour. The latter models have an oscillating path loss with decreasing spatial frequency and strong variations in the path gain occur as shown in figure 3.7.

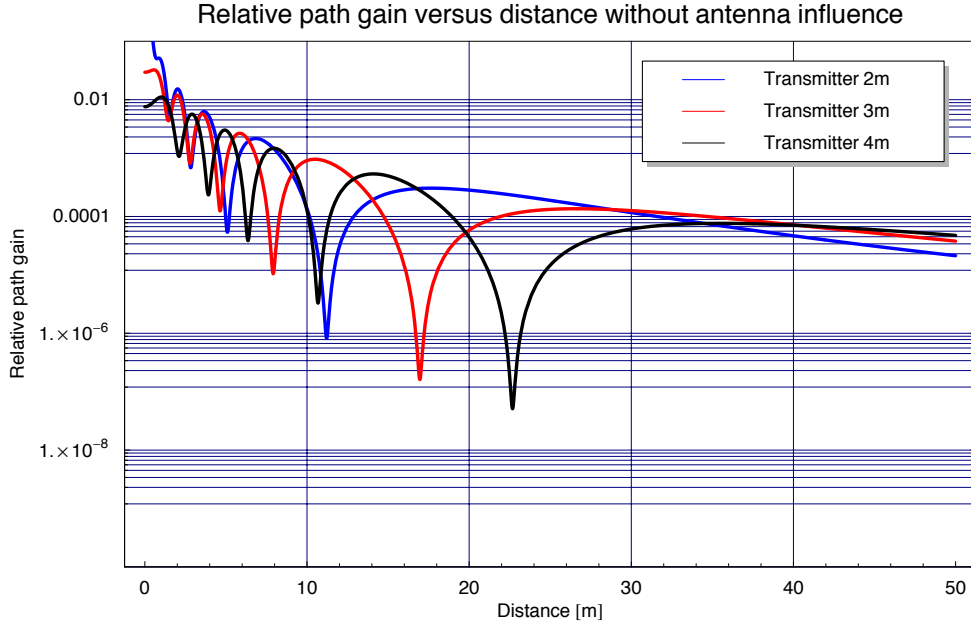


**Figure 3.7:** Relative path gain versus distance — Here shown for the two ray-model as presented in subsection 3.2 for a transmitter antenna height of 2 m, 3 m and 4 m, receiver antenna height 2 m, transmission frequency 434 MHz and vertical polarisation.

### Relative path gain for the two-ray model with antenna influence

The antenna radiation pattern may also be included in the multiple-ray model. Under the assumption that transmitter and receiver have the same type of antenna, the multiple ray model can be rewritten to include the antenna gain as

$$P_r(d) = P_t \left( \frac{\lambda}{4\pi} \right)^2 \left| \sum_{i=1}^N G_{a,i}^2 \frac{\Gamma_i(\alpha_i)}{r_i(d)} \exp(-ikr_i(d)) \right|^2 \quad (3.9)$$

$$k = \frac{2\pi}{\lambda} \quad N \dots \text{Number of rays}$$

where the notation  $G_{a,i}$  indicates that each ray undergoes an individual gain.

Figure 3.8 shows the relative path gain for the two ray model, but in this case includes the effect of the antenna radiation pattern for the short dipole. One fact to note in this figure is, that for small horizontal separations between the transmitter and the receiver, the effect of the antenna radiation pattern is very prominent. This is due to the fact that for larger separation distances the rays, the LOS and the ground reflected ray, are emitted at similar, small elevation angles, which in turn has the effect of a similar, higher gain. For

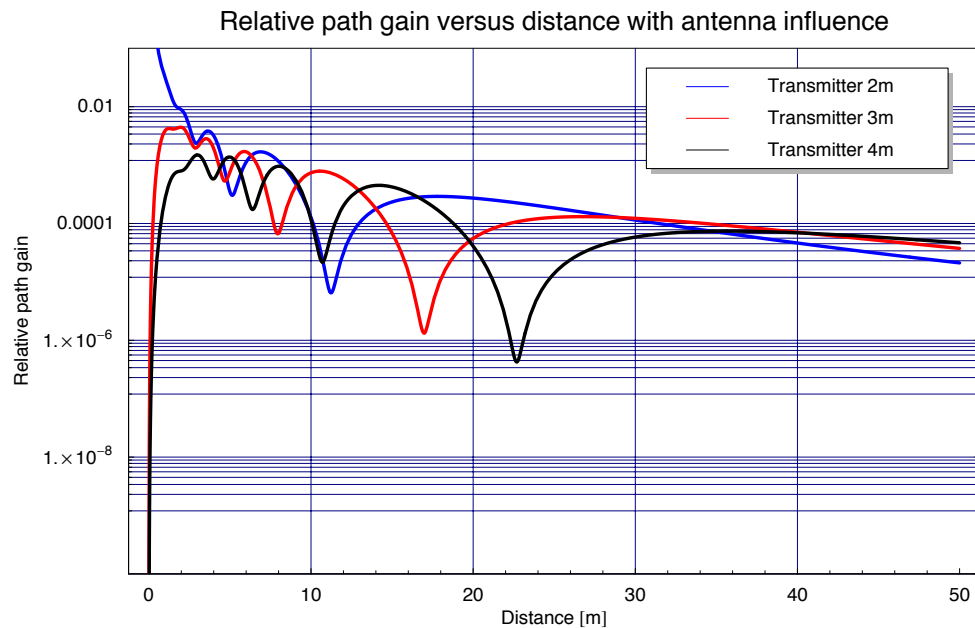


**Figure 3.8:** Relative path gain versus distance with antenna influence — This figure shows the relative path gain with the influence of the small dipole antenna pattern for a mounting height of 2 m, 3 m and 4 m for the transmitter antenna and a receiver antenna mounted at 2 m. The attenuation for small horizontal separation distances can be seen clearly and increases in magnitude with increased mounting height difference.

very short distances two cases are of interest. The first case is when both antennas are at similar heights and the second case is when they are separated vertically, i.e. mounted at different heights. In the first case, the LOS will have maximum gain as it is emitted at almost 90 degrees elevation angle, while the reflected ray will have almost minimum gain, as it is emitted at close to 180 degrees elevation angle. Therefore the LOS ray becomes dominant while the reflected ray has negligible impact. In the second case, the reflected ray will still have minimum gain as the angle of emission is still close to 180 degrees. But with increasing difference in the mounting height, the LOS ray will experience a decrease in the gain as the elevation angle increases. This leads to a very small signal at the receiver.

### The influence of the RF signal frequency

The frequency of the RF signal has an influence on the characteristic of the propagation pattern. Signals with higher frequency show a higher spatial oscillating behaviour than signals with a lower frequency, as can be seen in figure 3.9 for the frequencies of 434 MHz and 900 MHz.

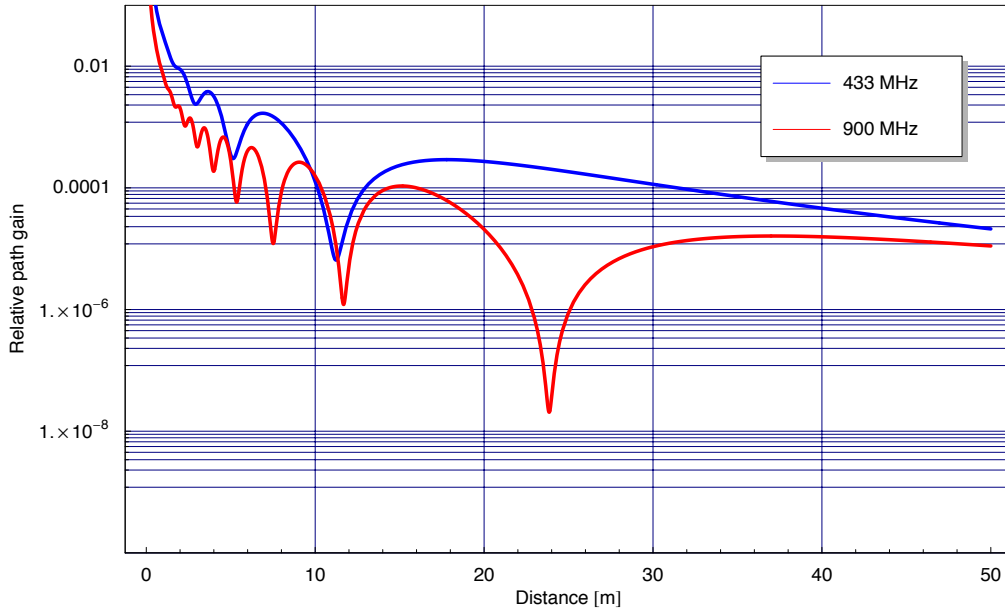


**Figure 3.9:** Relative path gain for two frequencies — Signals with higher frequency oscillate at a higher spatial frequency than signals with a lower frequency. Here shown is the case for transmitter and receiver heights of 2 m obtained using the two-ray model.

### 3.4.3 Communication models

This subsection presents some of the popular propagation models. The common denominator for these models is that they were developed to ensure area coverage. Area coverage is concerned with guaranteeing a signal quality (signal reception) within a given area. This is the primary task in communication. The models used are often built on empirical data.

#### General path loss model

The general description of the path loss in dBm, as a function of the distance  $d$ , is given as

$$PL(d) = PL(d_0) + 10\gamma \log(d/d_0) + \mathcal{X}_\sigma \quad (3.10)$$

In the above equation  $PL(d_0)$  denotes the reference path loss at distance  $d_0$ . The constant  $\gamma$  is called the path loss factor, and for  $\gamma = 2$  the above equation becomes the free space propagation loss (see also equation (3.1)). Different path loss factors are applicable to different environments and can either be found from tables or from experimental data. Using the Gaussian random variable  $\mathcal{X}_\sigma$  it is possible to model the uncertainty of the path loss. This model is also used for localisation applications and will be discussed at different points throughout this thesis with regards to its applicability for mobile robotics.

### Okomura et al. and Hata model

The Okomura model is a widely used outdoor propagation model for urban areas. It describes the median value of propagation path loss and can be written as

$$L_{50} = L_F + A_{mu}(f, d) - G(h_{te}) - G(h_{re}) - G_{Area} \quad (3.11)$$

In this equation  $L_F$  stands for the free space propagation loss, while  $A_{mu}$  is the median attenuation in the medium, relative to free space, at the frequency  $f$  and distance  $d$ . Furthermore, three gain factors for the transmitter  $G(h_{te})$ , the receiver antenna  $G(h_{re})$  and an area specific gain  $G_{Area}$  are included in this formula.  $A_{mu}$  and  $G_{Area}$  can be found using empirical curves.

The Hata model is a reduction of the many empirical curves obtained by Okomura et al. This model describes the median propagation loss in urban environments by

$$L_{50}(urban)(dB) = 69.55 + 26.16 \log f_c - 13.82 \log h_{te} - a(r_{re}) + (44.9 - 6.55 \log h_{te}) \log d \quad (3.12)$$

Here  $f_c$  is the transmission frequency in Megahertz (MHz) in the range from 150 MHz to 1500 MHz,  $h_{te}$  and  $h_{re}$  are the effective heights of the antennas of the transmitter and the receiver, respectively, and  $d$  is again the distance between both. The factor  $a(h_{re})$  is a correction factor for the effective antenna height of the mobile unit and is a function of the size of the area of coverage.

### Breakpoint or Dual-Slope models

Breakpoint models divide the distance domain  $d$  into two separate areas. This division occurs at the breakpoint  $d_{brk}$  and in each of these areas the path loss is described by its own equation with a different slope ( $n_1$  and  $n_2$  respectively), hence the names for this type of model.

$$PL(d) = PL_b + \begin{cases} 10n_1 \log d + P_1 & 1 < d < d_{brk}, \\ 10(n_1 - n_2) \log d_{brk} + 10n_2 \log d + P_1 & d \geq d_{brk} \end{cases} \quad (3.13)$$

The constant  $P_1$  represents the path loss at the reference distance  $d_0$ .  $PL_b$  is a transmission loss parameter dependent on the transmission frequency and the antenna heights.

### Indoor RF propagation modelling

Indoor propagation models often build on the general path loss model (equation (3.10)) and include additional factors for the attenuation as it might occur due to the walls (WAF) or floors (FAF) of the buildings.

$$PL(d) = PL(d_0) + 10\gamma \log(d/d_0) + \sum_{q=1}^Q \text{FAF}(q) + \sum_{p=1}^P \text{WAF}(p) \quad (3.14)$$

$Q, P \dots$  Number of floors/walls

### Ray-tracing techniques

Among the site-specific models the ray-tracing technique with its different extensions and levels of complexity is the most well-known. It is more prominent in the area of graphical visualisation, where realistic graphical representations of nature or objects are achieved. The underlying assumption that the radiated energy can be seen as rays traveling in straight lines (at least for a constant refractive index), is the same for the optical or the RF application. The ray-tracing technique launches rays from the transmitter and these rays interact with the environment according to the theory of refraction, reflection etc., or in general according to the theory of electromagnetic waves.

This technique is suitable to model indoor as well as outdoor propagation and is also capable of describing the small scale fading effects [60, 96].

Apart from the presented models, there are many other models used for communication purposes. The ITU (CCIR) model, the "Clearance Angle" model, the Ericsson Model 9999, the Lee Model, the Cost 231-Walfisch-Ikegami Model or the ETF-Artificial Neural Networks Macrocell Model [60] are named here to show the variety. The reader is referred to the communications literature for the details about these and other models.

#### 3.4.4 Robotics models

Several of the communication RF propagation models have been used for localisation and tracking purposes in mobile robotics, such as the indoor propagation model [8]. Other examples include the general path loss model [72] or the breakpoint model [82].

Some robotics-specific models have been developed for the task of localisation and tracking and a selection is described in this subsection.

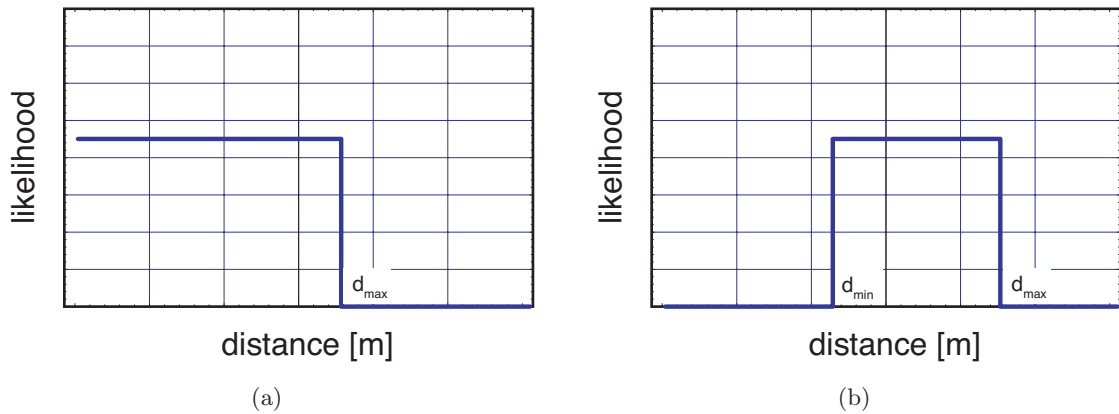


**Figure 3.10:** Binary and Distance-bound sensor models — (a) shows the binary model assigning equal likelihood to all distances smaller than a maximum distance  $d_{max}$ . (b) shows the distance bound model which assigns equal likelihood for distances within a certain range between  $d_{min}$  and  $d_{max}$ .

### Binary model and Distance bound model

Among the most simple sensor models, the binary model as used in robotics assigns equal likelihood for distances  $d < d_{max}$ , while the distance bound model does the same for the distance interval  $d_{min} < d < d_{max}$  (see figures 3.10(a) and (b)). One should note that these models assume omnidirectionality of the RF sensor, as they do not model any dependency on the azimuth angle. With this interval-type model accurate localisation is often not possible for obvious reasons, unless the density of nodes is high and their placement clever [19, 20].

### Discrete equal likelihood areas model

This model presented in [42] is one of the few models described in the area of mobile robotics that takes into account the antenna pattern and models the directionality of the antenna as shown in figure 3.11. Areas of detection are obtained from real data during a sensor modelling phase. Each area is assigned a discrete likelihood of detection.

### Signal strength maps

Signal strength maps, see figure 3.12, are used in indoor localisation and tracking applications. In these applications the mobile robot gathers RSSI information together with location information at the same time and so constructs a map of received signal strength [83]. During the localisation phase the received signal strength is matched against the map, and thus possible locations in the map are obtained. Subsequent observations obtained through motion in the mapped area will often eliminate multiple hypotheses.

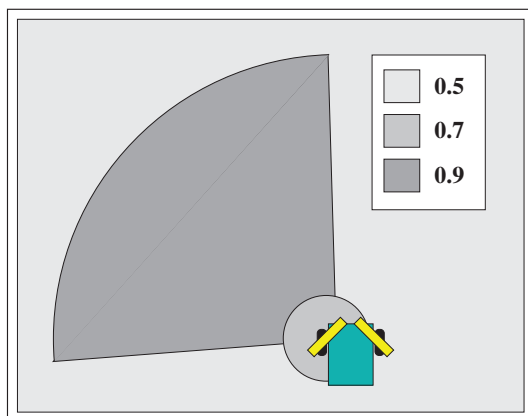


**Figure 3.11:** Discrete Equal Likelihood Areas Model — This model assigns discrete likelihoods to different areas which are distributed according to the antenna pattern. The picture is taken from [42].

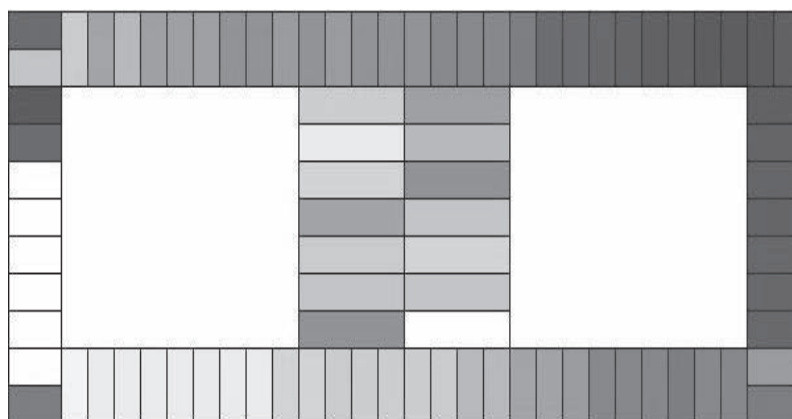


**Figure 3.12:** Signal strength map — This model creates a map of received signal strength from actual training data. The picture is taken from [83].

## 3.5 Summary

In this chapter the basics of RF propagation were presented. The main propagation mechanisms for electromagnetic waves were explained and the properties of antenna radiation patterns and their influence on the propagation were shown.

The majority of RF propagation models were developed for communication purposes and some of them were presented. Some of these models, for example the indoor propagation model, are used for localisation and tracking in mobile robotics.

Few models have been developed specifically for localisation and tracking in the field of mobile robotics. The models implemented to date have either modeled the fading effects at the large scale fading level, or they are even further simplified as is for example the Binary model. By neglecting the small scale fading effects and not modelling the signal mean at a more detailed level, it is not possible to achieve high-accuracy localisation using RF sensors. This issue will be discussed in the following chapters.